Achieving Scalable Near-Zero-Index Materials

Kevin J. Palm, Tao Gong, Calum Shelden, Ece Deniz, Lisa J. Krayer, Marina S. Leite, and Jeremy N. Munday*

Near-zero-index (NZI) materials are becoming increasingly important for photonic designs because they enable new ways to control light–matter interactions at the nanoscale. Many device prototypes that utilize NZI layers are created under conditions that are tool and laboratory specific, making widespread utilization and scalability of NZI materials difficult. Herein, this limitation is circumvented by using transparent conducting oxides (TCOs) produced from scalable commercial sources. The optical response of 49 distinct TCOs with NZI behavior from 12 different suppliers is quantified, including indium tin oxide (ITO), aluminum-doped zinc oxide (AZO), and fluorine-doped tin oxide (FTO). The measurements reveal that the ITO samples have the strongest NZI resonances with many samples exhibiting $|n| < 0.6$ with resonances occurring between 1150 and 1350 nm. Conversely, the FTO and AZO films present higher values of $|n|$ (ranging from 0.6 to 0.9) at 1500–1900 nm. The optical properties, resistivities, and roughness values for all thin films are reported, creating a useful database for device design. Finally, novel NZI phenomena, such as the strong suppression of non-normal incidence illumination using the data collected from these samples, are demonstrated, opening the door to new opportunities for both research-grade and mass-produced NZI devices.

1. Introduction

Near-zero-index (NZI) materials are becoming important elements for nanophotonic design and optical manipulation. As the name suggests, NZI occurs when the index of refraction of a material approaches zero over a certain wavelength range. This phenomenon is achieved when a conductive material has the real part of its permittivity cross zero combined with low Drude damping in the material (low loss). These properties allow for many extreme optical effects that stem from the phase velocity and wavelength approaching infinity as the index approaches zero, along with massive electric field enhancements within the material. Since the original seminal works on NZI materials,[1–3] there have been countless applications utilizing these novel properties. These applications range from creating various near-perfect absorption or transmission devices,[4–10] supercoupling light into narrow waveguides,[11–13] enhancing optical nonlinearities,[14–17] and increasing plasmonic effects,[18,19] among many others.

Transparent conducting oxides (TCOs) have become the most common NZI materials due to their broad NZI region located in the telecom wavelength range, low losses at the dielectric cross-over-point (where the real part of the dielectric function crosses zero), and tunability of the NZI wavelength based on deposition conditions. In particular, indium tin oxide (ITO),[14,17,18,20–23] aluminum-doped zinc oxide (AZO),[4,8,19,21,24] and fluorine-doped tin oxide (FTO)[25,26] have been well studied for their NZI properties and applications. While being a benefit in some cases, the large dependence of the optical properties of these materials on their deposition parameters can introduce difficulties in experimental replication, due to materials being deposited using different fabrication tools and methods across distinct institutions. As an example, the NZI resonance of ITO can vary from 1260 to 1920 nm depending on the annealing conditions.[27] This variability

K. J. Palm
Department of Physics
University of Maryland
College Park, MD 20742, USA

K. J. Palm, L. J. Krayer
Institute for Research in Electronics and Applied Physics
University of Maryland
College Park, MD 20742, USA

The ORCID identification number(s) for the author(s) of this article can be found under https://doi.org/10.1002/adpr.202200109.

T. Gong, C. Shelden, J. N. Munday
Department of Electrical and Computer Engineering
University of California
Davis, CA 95616, USA
E-mail: jnmunday@ucdavis.edu

T. Gong, E. Deniz, M. S. Leite
Department of Materials Science and Engineering
University of California
Davis, CA 95616, USA

L. J. Krayer
Department of Electrical and Computer Engineering
University of Maryland
College Park, MD 20742, USA

results from modifications in the carrier concentration within the material and completely changes the device performance.

Additionally, there are many commercial companies that sell TCO materials on substrates that can be used for NZI applications. By being able to purchase from one of these suppliers, the fabrication issues from batch to batch along with comparisons across different tools are eliminated. Here, we present a universal database of the optical properties of 49 commercial TCO samples and report the existence, strength, and width of their NZI resonances, all using comparable optical models. We characterize different types of TCOs: ITO, FTO, and AZO from a total of 12 different suppliers. Beyond their optical properties, we also determine the thickness, resistivity, and roughness for all the measured samples, providing a comprehensive library of the relevant properties needed for the design of NZI-based photonic devices. Using these measured properties, we find general correlations relating the optical and electrical properties of these materials. We demonstrate that both the strength and the bandwidth of an NZI resonance are correlated with the location of the resonance and that the strength of the resonance is loosely correlated with the resistivity of the TCO film. We find no strong relation between the roughness and optical properties of the films. Our results provide a resource for the development of novel NZI devices based on repeatable and comparable NZI materials, overall representing a pathway for mass-produced photonic devices based on these materials.

2. Measurement and Optical Modeling

To measure the optical properties of the samples, we use variable-angle spectroscopic ellipsometry (Woollam M-2000). We acquire reflection measurements of each sample at 65°, 70°, and 75°, and use the same tool to make normal incidence transmission measurements. The raw optical data are fit using a general oscillator model with one Drude oscillator[28] and up to three Tauc–Lorentz oscillators.[29] The number of Tauc–Lorentz oscillators is determined by only adding a further oscillator to the model if this addition causes a $> 10\%$ decrease in the mean-squared error (MSE) of the fit. This method is used to avoid over-fitting the data with spurious resonances. For each sample where the company provided a bare substrate without the TCO deposited, the optical properties of the substrate are measured separately, and these properties were input into the model fitting the TCO data. For samples where the suppliers that did not provide a substrate, we use the material properties from the Woollam database for the substrates (soda-lime glass, float glass, or glass slide dependent on which one was used) in our fits. Our fits also accounted for reflections from the backside of the substrate. The thickness of the TCO films is determined from the optical fitting, with the transmission intensity data allowing us to unambiguously determine its value. For a complete description of each of the fitting parameters, see the Supporting Information.

Instead of having a single layer of TCO, many of the FTO samples are multilayer structures, which is incorporated into the fitting model. On top of the glass substrates, a thin layer of SnO_2 was deposited, followed by a thin SiO_2 layer, and finally the active FTO layer. Here, we only report the optical properties of the top active FTO layer. In our optical model, we define the optical properties of the SnO_2 with a Cauchy model and define the properties of the SiO_2 layer with experimental data from sputtered SiO_2. In the model fit, we fit the thicknesses of these two intermediary layers and the thickness of the top FTO layer, along with the oscillator values defining the properties of the FTO. These two added fit parameters add extra variance to our fits, causing a larger error in the reporting of these FTO properties. Two of the FTO samples, sourced from Biotain Crystal and MSE Supplies, are both single-layer samples and, thus, are fit using the same process as the ITO and AZO samples detailed above.

3. Properties of TCO Films

Typical results for the optical properties of ITO, FTO, and AZO are shown in **Figure 1**. Although there can be fairly large variations from sample to sample, data from each material generally follow the same overall trends. In general, ITO displays a strong NZI resonance between 1150 and 1400 nm with a higher index of refraction in the visible range of the electromagnetic spectrum and higher attenuation further into the infrared (IR). FTO usually shows a much weaker resonance than ITO, and this NZI resonance is located >1690 nm. This same trend holds with AZO. In the short wavelength range (≈ 400 nm), AZO also exhibits a peak in attenuation. For the individual optical properties, company names, and nominal resistances for each of the 49 samples
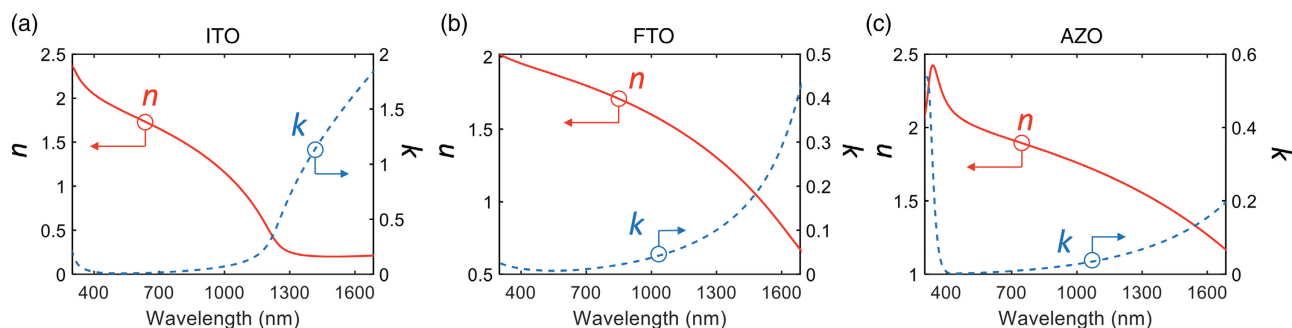

Figure 1. Optical properties of typical a) ITO, b) FTO, and c) AZO films. The real (n) and imaginary (k) parts of the refractive index are represented by a solid red and a dashed blue line, respectively. This data shows the general trends for each type of material; yet, fabrication conditions can lead to significant variations in n,k.
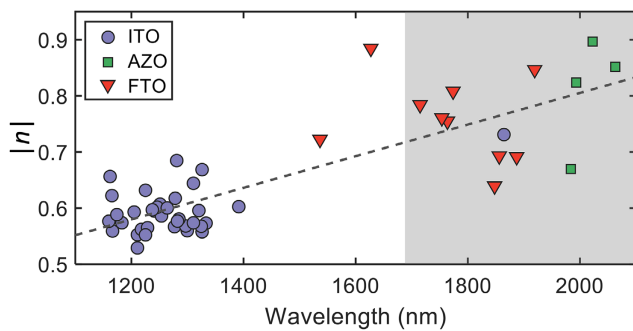
Figure 2. Magnitude of the minimum index of refraction for each TCO, $|n| = \sqrt{n^2 + k^2}$, plotted against the wavelength where this minimum occurs. The gray shaded region shows extrapolated data of the oscillator fits obtained from the experimental region (up to 1690 nm). ITO samples are shown as purple circles, AZO as green squares, and FTO as red triangles. The dashed gray line is a linear fit to the data to draw attention to the positive correlation.

reported, see Figure S1–S5, Supporting Information. The fitted Ψ, Δ, and transmission ellipsometry data for these samples can be found in Figure S6–S10, Supporting Information, and all the oscillator fitting parameters can be found in Table S1, Supporting Information.

Figure 2 displays the minimum magnitude of the refractive index, $|n| = \sqrt{n^2 + k^2}$, versus the wavelength where that minimum is found. Lower $|n|$ allows for stronger NZI effects, such as larger electric field enhancements, wider diverging phase and group velocities, and larger wavelength expansions.[30] In the plot, the gray shaded region denotes extrapolated data as the range of our optical measurement ends at 1690 nm. For data in this region, we extrapolate the optical properties using the oscillators defined from fitting the ellipsometric data. We note that if there are additional phononic resonances or additional bound electron resonances in this region, it could further affect the optical properties in unaccounted ways, adding a higher uncertainty for values in this region. The further away the resonance is from the maximum measurement wavelength of

1690 nm, the higher the uncertainty is in the resonance strength and location.

Our measurements reveal two general trends in the NZI resonances. First, the three different materials have NZI resonances that occur in slightly different parts of the spectrum. The center wavelength for the ITO NZI resonance occurs in the ≈1100–1400 nm range (except for one outlier). As we traverse further into the IR, we find the region containing the FTO resonances (≈1500–1900 nm), and finally, the region where the AZO resonances can be found (≈1950–2100 nm). The second trend that we find is that the strongest NZI resonances (e.g., lowest $|n|$) occur at shorter wavelengths. As the wavelengths extend further into IR, the resonances become slightly weaker. We fit a linear trend line to this plot to show this relationship.

The bandwidth of the resonance (hereby defined as the width of the spectral region where $|n| < 1$) is also of vital importance for broadband devices required to perform at many wavelengths, such as broadband absorbers[5,8,9] and transmission devices.[7,10] In **Figure 3**, we plot the bandwidth of the NZI resonance for each of our measured materials versus the location of the center wavelength of the NZI resonance (location of the minimal $|n|$ value). We find that as the location of the resonance shifts into the IR, the bandwidth increases while its strength decreases. The gray shaded region in this figure depicts the region where the center wavelength of the NZI resonance is found by extrapolation. We also note that in this figure, the two FTO samples whose center wavelengths are located in the measured region also involve some extrapolation, as the region where $|n| < 1$ extends beyond our maximum measured wavelength of 1690 nm. For the materials that do involve extrapolation, we find a much wider range in results deviating from our linear trend line. In this study, we cannot determine whether this high variance effect is caused by additional error from the extrapolation, differences in material responses (as most of these materials are FTO and AZO), or if materials with NZI resonances in this regime behave differently. In all likelihood, it is some combination of these three factors. Figure 3b shows the same plot with only the data with no extrapolation, which happens to entirely consist of ITO samples. This trend is positive, with most of the data points supporting the
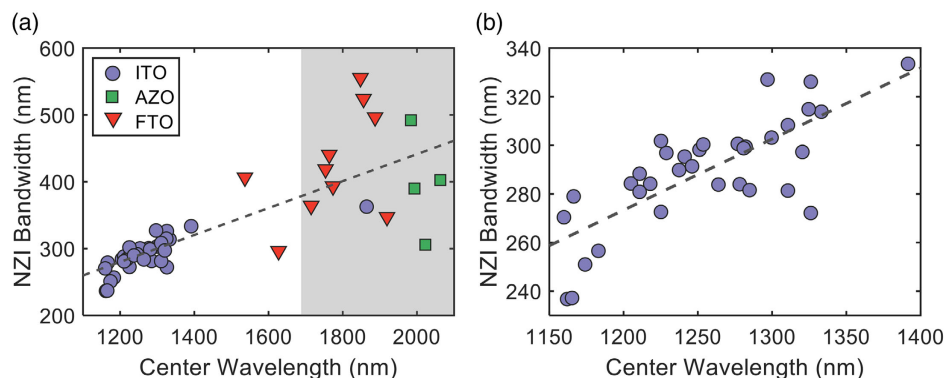

Figure 3. a) Bandwidth of NZI resonance versus the center wavelength of the resonance. We find that as the NZI wavelength moves further into the infrared, the bandwidth of the NZI increases. Bandwidth is defined as the size of the wavelength region where $|n| < 1$. ITO samples are shown as purple circles, AZO as green squares, and FTO as red triangles. The gray dashed line is a linear fit to the data to guide the eye of the reader. b) Data for samples that involved no extrapolation in the bandwidth.
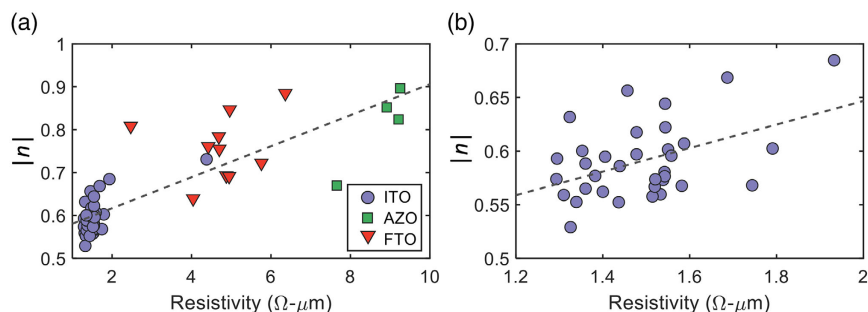
(a)

(b)

Figure 4. a) Minimum index of refraction versus the resistivity of each TCO film showing that generally as the resistivity of the film increases, so does the minimum magnitude of the index of refraction. ITO samples are shown as purple circles, AZO as green squares, and FTO as red triangles. The gray dashed line is a linear fit to the data to guide the eye of the reader. b) Data for samples that require no extrapolation in the optical properties.

conclusion that materials with NZI resonances at longer wavelengths have a broader resonance bandwidth.

The positive correlation between the center wavelength and the bandwidth of the NZI region, combined with the correlation between the strength (i.e., minimum $|n|$) and wavelength, creates a trade-off in device design. By choosing a sample with a resonance closer to the visible regime, we can achieve a stronger resonance, but at the cost of a smaller bandwidth. Thus, for some applications, the ideal material might present a resonance further into the IR, where a fairly strong resonance can still be achieved, and a more broadband effect is possible.

For each sample, we acquire 4-point probe resistivity measurements to characterize the electrical properties of the TCO films. Here, we use a Signatone 4-point probe device readout with a Keithley 2400 sourcemeter. The dimensions of each sample measured are large enough that no size compensation had to be applied to the sample measurement. Each sample is measured in three different orientations near the center of the sample, and the results reported are the averages of these measurements. In **Figure 4**, we show the resistivity of each TCO film versus the minimum $|n|$. We find that as the resistivity of the films increases, $|n|$ also increases. This correlation is in agreement with the literature, where it has been found that higher carrier concentrations in ITO samples lead to stronger NZI resonances with these resonances located at shorter wavelengths.[27] We find that FTO and AZO films have higher resistivities than the ITO films, requiring their films to be much thicker to obtain similar sheet resistance values. For samples where a thin coating is

required with high conductivity, ITO seems to be the only available commercial option of the three materials we investigated. In Figure 4b, we isolate the unextrapolated ITO samples and find a similar correlation over a smaller scale, with all the resistivities of these samples located between 1.2 and 2 $\Omega\,\mu m$.

To characterize the morphology and roughness of all TCOs, we use contact-mode atomic force microscopy (AFM) (Asylum MFP-3D system). The reported roughnesses are all root-mean-square (RMS) roughness and are calculated by taking the RMS values of each line of the AFM image and then the median of these values. **Figure 5** shows the minimum index of refraction $|n|$ versus RMS roughness. Note that there is little correlation between the overall roughness of the samples and the optical properties. The FTO and AZO samples are slightly rougher than ITO, with RMS values >10 nm. This result suggests that significantly rougher films may lead to additional optical loss and, hence, reduced NZI effects.

Table 1 summarizes the complete findings of the optical, electrical, and topographic measurements for all 49 TCOs. We purposely chose samples from 12 distinct suppliers to demonstrate the wide range of overall optical behavior and that strong NZI responses can be obtained from many sources. Overall, the nominal resistivity provided by the suppliers agrees well with our measured values and is a useful quantity to identify each sample due to its correlation with $|n|$. Concerning film thickness, a variation ranging from 30 to >800 nm can be found commercially, which allows for a wide range of devices, as some devices require thin films of NZIs,[8,9] while others require thick films to obtain
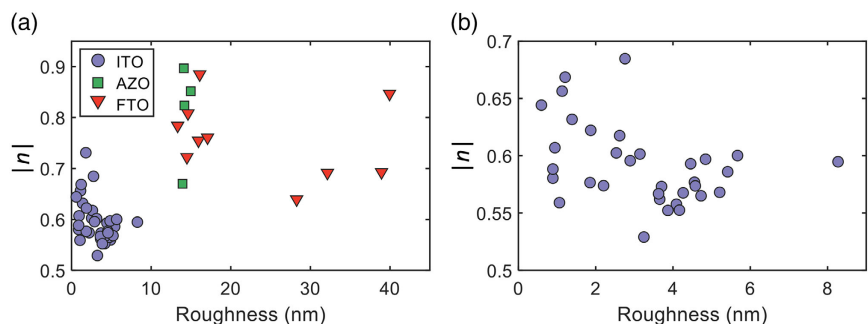
(a)

(b)

Figure 5. a) Minimum index of refraction versus the root mean square roughness of TCO films. We find little correlation between the roughness of the samples and the strength of their NZI resonance. ITO samples are shown as purple circles, AZO as green squares, and FTO as red triangles. b) Data for samples that require no extrapolation in the optical properties.

ADVANCED
SCIENCE NEWS

www.advancedsciencenews.com

ADVANCED
PHOTONICS
RESEARCH
Open Access

www.adpr-journal.com

Table 1. Summary of properties of all measured samples. Nominal R is resistance quoted by company, R is the measured resistance, t is the optically determined film thickness, $|n|$ is the minimum magnitude of the index of refraction, λ is the location of that minimum, $\Delta\lambda$ is the bandwidth of the region where $|n| < 1$, and τ is the measured RMS roughness of the sample. Suppliers are: 1) Adafruit Industries, 2) Biotain Crystal, 3) Delta Technologies, 4) MSE Supplies, 5) MTI Corporation, 6) NanoCS, 7) Nanoshel, 8), Ossila, 9) SPI, 10) Sigma-Aldrich, 11) Techinstro, and 12) University Wafer.

Supplier	Material	Nominal R [Ω sq^{-1}]	R [Ω sq^{-1}]	t [nm]	$|n|$	λ [nm]	$\Delta\lambda$ [nm]	τ [nm]
1	ITO	10–15	8.45	181.5	0.56	1300	303	4.9
2	AZO	8–10	8.35	916.8	0.67	1984	492	13.9
2	FTO	10–15	15.06	382.3	0.72	1536	406	14.5
2	ITO	10–15	11.15	138	0.57	1333	314	3.7
2	ITO	30–40	23.15	56.6	0.56	1166	279	1.1
2	ITO	4–5	6.09	212.7	0.59	1205	284	4.5
2	ITO	6–8	8.38	180.7	0.56	1326	326	4.1
2	ITO	80–100	76.27	19.1	0.66	1162	237	1.1
3	FTO	16–20	19.96	234.8	0.78	1715	364	13.3
3	ITO	15–25	19.61	67.5	0.63	1225	273	1.4
3	ITO	30–60	44.29	29.2	0.57	1183	257	2.2
3	ITO	4–8	8.43	158.9	0.55	1211	288	4.2
3	ITO	8–12	11.55	121.2	0.56	1218	284	3.7
4	AZO	10	10.60	869	0.82	1993	390	14.2
4	FTO	15	20.72	307	0.88	1627	296	16.1
4	ITO	12–15	13.43	133.4	0.60	1392	334	2.5
4	ITO	30	34.28	46.3	0.61	1251	298	0.9
4	ITO	3–5	3.97	354	0.59	1241	295	8.3
4	ITO	7–10	5.99	227.1	0.57	1229	297	4.7
5	ITO	12–15	11.09	142.6	0.57	1325	315	4.3
5	ITO	16–19	14.22	106.9	0.57	1277	301	3.6
5	ITO	6–7	6.47	222.6	0.59	1254	300	5.4
5	ITO	8–10	9.37	186.1	0.57	1297	327	5.2
6	FTO	12–17	7.08	349.1	0.81	1774	393	14.6
6	ITO	100	78.09	21.6	0.67	1326	272	1.2
6	ITO	10	7.59	174.8	0.53	1211	281	3.1
6	ITO	20	15.69	94.2	0.62	1278	284	2.6
6	ITO	50	41.91	36.8	0.58	1285	282	0.9
6	ITO	5	3.91	354	0.58	1282	299	4.5
7	AZO	10	10.10	891.3	0.85	2063	402	15.0
7	ITO	10	8.38	185	0.60	1246	291	3.1
7	ITO	15	25.06	61.7	0.58	1160	270	1.8
8	FTO	11–13	11.33	437.9	0.85	1919	347	39.9
8	FTO	12–14	13.22	355.5	0.75	1764	440	15.9
8	FTO	6–9	7.80	625	0.69	1856	524	38.9
8	ITO	20	17.34	111.5	0.68	1281	299	2.8
9	ITO	30–60	34.62	126.5	0.73	1864	363	1.8
10	FTO	8	8.20	603.1	0.69	1887	497	32.1
10	ITO	30–60	45.04	30.2	0.59	1174	251	0.9
10	ITO	70–100	85.31	18.1	0.62	1165	237	1.9
10	ITO	8–12	11.64	123.4	0.55	1225	302	3.9
11	AZO	10	11.03	838.6	0.90	2023	306	14.1
11	FTO	15	12.89	343	0.76	1754	419	17.1
11	FTO	7	7.03	574.4	0.64	1848	555	28.3

**ADVANCED
SCIENCE NEWS**

www.advancedsciencenews.com

**ADVANCED
PHOTONICS
RESEARCH**
Open Access

www.adpr-journal.com

Table 1. Continued.

Supplier	Material	Nominal R [Ω sq^{-1}]	R [Ω sq^{-1}]	t [nm]	$|n|$	λ [nm]	$\Delta\lambda$ [nm]	τ [nm]
11	ITO	100	83.43	18.5	0.64	1311	281	0.6
11	ITO	10	8.05	183.5	0.60	1237	290	4.8
11	ITO	20	10.24	148.5	0.57	1311	308	4.6
12	ITO	15–20	15.42	101	0.60	1320	297	2.9
12	ITO	7	6.34	213.3	0.60	1264	284	5.7

the desired effect.[5] Because the design of NZI devices heavily relies on controlling the wavelength of minimum magnitude of $|n|$ (and, thus, strong resonance), the table also displays their precise values, combined with the bandwidth where $|n| < 1$. As expected, the position of maximum resonance lies beyond the visible range of the spectrum for all TCOs. As mentioned earlier, most films present roughness <10 nm (for AFM images, see Figure S6–S10, Supporting Information).

Finally, we show that novel NZI phenomena can be demonstrated with the samples described above. As an example, **Figure 6** shows the strong suppression of non-normal incidence illumination at the NZI frequency, a phenomenon first predicted in 2007.[31] When an electromagnetic plane wave (TM-polarized) is incident on a thin film of an ideal NZI material ($n = 0$), no transmission occurs through the film except at normal incidence (incidence angle $\theta = 0$), i.e., the transmission features a delta function-like resonance with respect to θ. If the index of refraction deviates from the zero, as with the real materials, the resonance either occurs at a small incidence

angle at $\theta = \sin^{-1}(n)$ (if n has a small positive value) or features a broader angular dependence (if the loss is nontrivial). Here, we use the dielectric function of one of our measured ITO samples (supplier 10; ITO; 70–100 Ω) to probe this effect. Figure 6 shows the transmission spectra with respect to wavelength and incidence angle calculated using the transfer matrix method for (a) an ideal NZI material, whose dielectric function is described using a Drude model with the plasma wavelength $\lambda_P = 1.17\,\mu$m and zero damping, and (b) the real ITO sample data. Two observations can be made. First, for TE polarization, the transmission falls off slowly with incidence angle for any wavelength of interest; whereas for TM polarization, the transmission drops much more rapidly at the NZI wavelength, as expected for this angular filtering effect. Second, the loss in the ITO material does broaden the angular distribution of transmission at the NZI wavelength; however, this effect is still significant when compared to any other (non-NZI) wavelengths. Overall, this result exemplifies the viability of realizing NZI effects using commercial ITO materials.
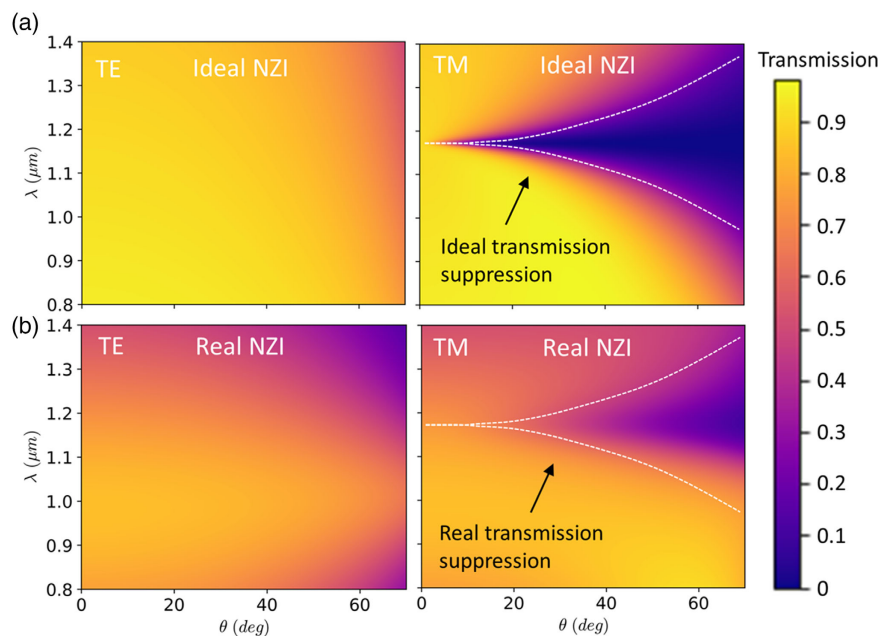

Figure 6. Contour plots of the transmission spectra through a thin NZI slab (100 nm thick) at varying angles of incidence. a) Ideal NZI material using a Drude model with $\lambda_p = 1.17\,\mu$m and $\gamma_p = 0$. b) Real ITO corresponding to the measured optical data from one of the samples from supplier 10 (70–100 Ω) with the NZI wavelength of $\approx 1.17\,\mu$m. The transmission of TM polarization drops substantially with increasing angle of incidence, as expected due to the NZI behavior. The drop is less pronounced for the real NZI material because of the optical loss, but is still clearly visible. Dotted lines are a guide-to-the-eye showing the region of transmission suppression.

4. Conclusion

In conclusion, we have developed a universal library for NZI materials by determining the optical, electrical, and topographical properties of 49 different TCO samples and have found a wide range of NZI properties. We found that ITO is the most readily available NZI material, with many different samples having $|n| < 0.6$. Through this comprehensive analysis, we demonstrated novel NZI-behavior, e.g., strong suppression of non-normal incidence illumination, opening the door to new opportunities for both research-grade and mass-produced NZI devices. We also identified a correlation between the location of the NZI resonance and the strength and bandwidth of that resonance, with shorter wavelengths leading to stronger resonances with a smaller bandwidth and longer wavelengths leading to weaker resonances with a wider bandwidth. We found a loose correlation between the strength of the NZI behavior and the resistivity of the TCO films, with a lower resistivity leading to a slightly stronger NZI response and found no significant relationship between a film's topographical roughness and its optical properties. Our results show the breadth and availability of different TCO materials for NZI applications, allowing our database to be used by researchers designing novel, scalable photonic devices based on NZI phenomena.

Supporting Information

Supporting Information is available from the Wiley Online Library or from the author.

Acknowledgements

Conflict of Interest

The authors declare no conflict of interest.

Data Availability Statement

The data that support the findings of this study are available from the corresponding author upon reasonable request.

Keywords

[1] S. Enoch, G. Tayeb, P. Sabouroux, N. Guérin, P. Vincent, *Phys. Rev. Lett.* **2002**, *89*, 213902.
[2] N. Garcia, E. V. Ponizovskaya, J. Q. Xiao, *Appl. Phys. Lett.* **2002**, *80*, 1120.
[3] R. W. Ziolkowski, *Phys. Rev. E* **2004**, *70*, 046608.
[4] L. J. Krayer, J. Kim, J. L. Garrett, J. N. Munday, *ACS Photonics* **2019**, *6*, 2238.
[5] L. J. Krayer, J. Kim, J. N. Munday, *Opt. Mater. Express* **2019**, *9*, 330.
[6] S. Vassant, A. Archambault, F. Marquier, F. Pardo, U. Gennser, A. Cavanna, J. L. Pelouard, J. J. Greffet, *Phys. Rev. Lett.* **2012**, *109*, 237401.
[7] V. C. Nguyen, L. Chen, K. Halterman, *Phys. Rev. Lett.* **2010**, *105*, 233908.
[8] J. Rensberg, Y. Zhou, S. Richter, C. Wan, S. Zhang, P. Schöppe, R. Schmidt-Grund, S. Ramanathan, F. Capasso, M. A. Kats, C. Ronning, *Phys. Rev. Appl.* **2017**, *8*, 014009.
[9] S. Feng, K. Halterman, *Phys. Rev. B* **2012**, *86*, 165103.
[10] K. Halterman, S. Feng, *Phys. Rev. A* **2008**, *78*, 021805.
[11] A. Alù, M. G. Silveirinha, N. Engheta, *Phys. Rev. E* **2008**, *78*, 016604.
[12] B. Edwards, A. Alù, M. E. Young, M. Silveirinha, N. Engheta, *Phys. Rev. Lett.* **2008**, *100*, 033903.
[13] D. C. Adams, S. Inampudi, T. Ribaudo, D. Slocum, S. Vangala, N. A. Kuhta, W. D. Goodhue, V. A. Podolskiy, D. Wasserman, *Phys. Rev. Lett.* **2011**, *107*, 133901.
[14] A. Capretti, Y. Wang, N. Engheta, L. D. Negro, *Opt. Lett.* **2015**, *40*, 1500.
[15] C. Argyropoulos, P.-Y. Chen, G. D'Aguanno, N. Engheta, A. Alù, *Phys. Rev. B* **2012**, *85*, 045129.
[16] H. Suchowski, K. O'Brien, Z. J. Wong, A. Salandrino, X. Yin, X. Zhang, *Science* **2013**, *342*, 1223.
[17] M. Z. Alam, I. D. Leon, R. W. Boyd, *Science* **2016**, *352*, 795.
[18] D. Traviss, R. Bruck, B. Mills, M. Abb, O. L. Muskens, *Appl. Phys. Lett.* **2013**, *102*, 121112.
[19] J. Kim, A. Dutta, G. V. Naik, A. J. Giles, F. J. Bezares, C. T. Ellis, J. G. Tischler, A. M. Mahmoud, H. Caglayan, O. J. Glembocki, A. V. Kildishev, J. D. Caldwell, A. Boltasseva, N. Engheta, *Optica* **2016**, *3*, 339.
[20] Z. Ma, Z. Li, K. Liu, C. Ye, V. J. Sorger, *Nanophotonics* **2015**, *1*, 198.
[21] G. V. Naik, J. Kim, A. Boltasseva, *Opt. Mater. Express* **2011**, *1*, 1090.
[22] S. Campione, I. Kim, D. de Ceglia, G. A. Keeler, T. S. Luk, *Opt. Express* **2016**, *24*, 18782.
[23] S. Campione, J. R. Wendt, G. A. Keeler, T. S. Luk, *ACS Photonics* **2016**, *3*, 293.
[24] N. Kinsey, C. DeVault, J. Kim, M. Ferrera, V. M. Shalaev, A. Boltasseva, *Optica* **2015**, *2*, 616.
[25] F. J. Gonzalez, R. E. Peale, S. Benis, D. Hagan, E. Van Stryland, in *2019 IEEE Res. Appl. Photonics Def. Conf. RAPID*, IEEE, Piscataway, NJ **2019**, pp. 1–3.
[26] F. Khalilzadeh-Rezaie, I. O. Oladeji, J. W. Cleary, N. Nader, J. Nath, I. Rezadad, R. E. Peale, *Opt. Mater. Express* **2015**, *5*, 2184.
[27] H. Zhao, Y. Wang, A. Capretti, L. Dal Negro, J. Klamkin, *IEEE J. Sel. Top. Quantum Electron.* **2015**, *21*, 192.
[28] T. E. Tiwald, D. W. Thompson, J. A. Woollam, W. Paulson, R. Hance, *Thin Solid Films* **1998**, *313–314*, 661.
[29] G. E. Jellison, F. A. Modine, *Appl. Phys. Lett.* **1996**, *69*, 371.
[30] N. Kinsey, C. DeVault, A. Boltasseva, V. M. Shalaev, *Nat. Rev. Mater.* **2019**, *4*, 742.
[31] A. Alù, M. G. Silveirinha, A. Salandrino, N. Engheta, *Phys. Rev. B* **2007**, *75*, 155410.